The MU radar with an active phased array system
1. Antenna and power amplifiers

Shoichiro Fukao,[1,2] *Toru Sato,*[3] *Toshitaka Tsuda,*[3] *Susumu Kato,*[3] *Koichiro Wakasugi,*[4] *and Tsuneichi Makihira*[5]

Reprinted from
RADIO SCIENCE
Volume 20 Number 6 November/December 1985

Radio Science, Volume 20, Number 6, Pages 1155–1168, November–December 1985

The MU radar with an active phased array system 1. Antenna and power amplifiers

Shoichiro Fukao,[1,2] *Toru Sato*,[3] *Toshitaka Tsuda*,[3] *Susumu Kato*,[3] *Koichiro Wakasugi*,[4] *and Tsuneichi Makihira*[5]

(Received February 14, 1985; revised June 11, 1985; accepted June 26, 1985.)

The MU (middle and upper atmosphere) radar of Japan is a 46.5-MHz pulse-modulated monostatic Doppler radar with an active phased array system. The nominal beam width is 3.6° and the peak radiation power is 1 MW with maximum average power of 50 kW. The system is composed of 475 crossed three-subelement yagi antennas and an equivalent number of solid state power amplifiers (transmitter-receiver modules). Each yagi antenna is driven by a transmitter-receiver module with peak output power of 2.4 kW. This system configuration enables very fast and almost continuous beam steering that has not been realized by other mesosphere-stratosphere-troposphere radars. Also, a variety of sophisticated operations are made feasible by dividing the antenna array into several independent subarrays. A brief description of the system, particularly its antenna and power amplifiers, is presented herein.

1. INTRODUCTION

The sensitive VHF/UHF band Doppler radars known as mesosphere-stratosphere-troposphere (MST) radars are powerful tools for the investigation of various dynamic processes occurring in both the middle atmosphere (altitude range 10–100 km) and the lower atmosphere except near the planetary boundary layer (about 2–10 km). The wide-ranging results obtained to date by means of this equipment will not be restated; readers are referred to the extensive review papers by *Balsley and Gage* [1980, 1982], *Gage and Balsley*, [1984], *Green et al.* [1979], *Harper and Gordon* [1980], *Larsen and Röttger* [1982], and *Röttger* [1984].

This type of radar, operating in the VHF band, was completed in November 1984 at Shigaraki, Shiga, Japan (34.85°N, 136.10°E), by the Radio Atmospheric Science Center of Kyoto University [*Kato et al.*, 1984]. This radar has been named "MU radar" in reference to the middle and upper atmosphere, which are the system's principal objects of investigation.

The most outstanding feature of the MU radar is an active phased array system [*Fukao et al.*, 1980]. It is the first MST radar to employ such a system. In conventional radar systems a high-power transmitter feeds all array elements via an appropriate cascading feeding network. The MU radar system, on the other hand, does not incorporate such a passive array connected to a high-power transmitter. Instead, each element of the phased array is provided with a low-power amplifier, and all the amplifiers are coherently driven by low-level pulses in order to produce the desired peak output power. The two systems are contrasted in Figure 1.

This system configuration enables very fast and almost continuous beam steering as well as various flexible operations made possible by dividing the antenna array into independent subarrays. These capabilities, which are the result of the low signal levels at which phase shift and signal division/combination are carried out by electronic devices, are expected to fulfill the principal research requirement; that is, the MU radar enables a pioneering study of the three-dimensional structures of atmospheric waves and turbulence in mesoscale and microscale. To date, this kind of study has rarely been performed in the middle atmosphere with the exception of a short-term mesospheric observation by the SOUSY MST radar [*Klostermeyer and Rüster*, 1984].

The outline of the MU radar system and a few

[1]Department of Electrical Engineering, Kyoto University, Yoshida, Japan.
[2]Now at Radio Atmospheric Science Center, Kyoto University.
[3]Radio Atmospheric Science Center, Kyoto University, Uji, Japan.
[4]Department of Electrical Engineering, Kyoto Institute of Technology, Matsugasaki, Japan.
[5]Communication Equipment Works, Mitsubishi Electric Corporation, Amagasaki, Hyogo, Japan.

Paper number 5S0523.
0048-6604/85/005S-0523$08.00

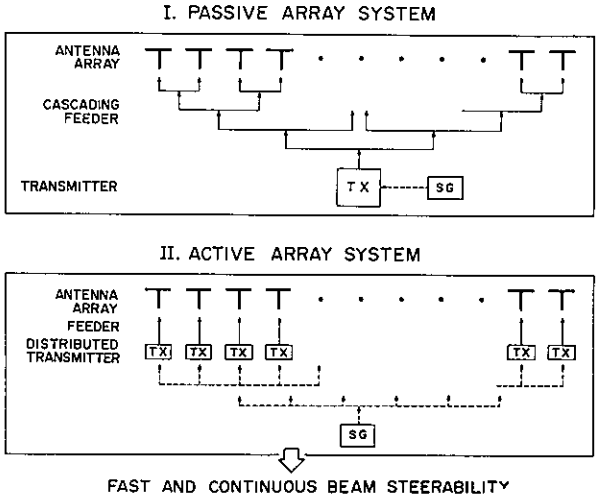

Fig. 1. A schematic diagram of passive and active phased array systems.

preliminary results using a partial system are presented by *Kato et al.* [1984]. This paper focusses on the hardware, especially on the antenna and power amplifiers adopted to realize the unique active array system of the MU radar. Other in-house equipment is briefly described in the accompanying paper [*Fukao et al.*, this issue].

2. SYSTEM OUTLINE

The MU radar is a monostatic radar with an active phased array system. The operational frequency is 46.5 MHz and the maximum peak and average radiation powers are 1 MW and 50 kW, respectively. The antenna is a circular array with an aperture of 8330 m^2. The nominal beam width is 3.6°. The shortest 1-μs pulse width is available in the 1.65-MHz bandwidth reserved exclusively for the MU radar. Figure 2 shows a general block diagram of the MU radar system (same as Figure 1 of *Kato et al.* [1984]). The basic parameters of the MU radar are given in Table 1.

This system is composed of 475 array elements and an identical number of transmitter-receiver (TR) modules [*Fukao et al.*, 1980; *Kato et al.*, 1984]. The TR modules are accommodated in six TR booths near the antenna array. The whole system can be divided into 25 groups (i.e., one group consists of 19 array elements and 19 TR modules). Each array element is driven by its own TR module. The main constituents of the TR module are a solid state transmitter, a receiver preamplifier, a T/R switch, and a digital phase shifter.

Both the upconvert from and the downconvert to the intermediate frequency (IF) of 5 MHz are per-

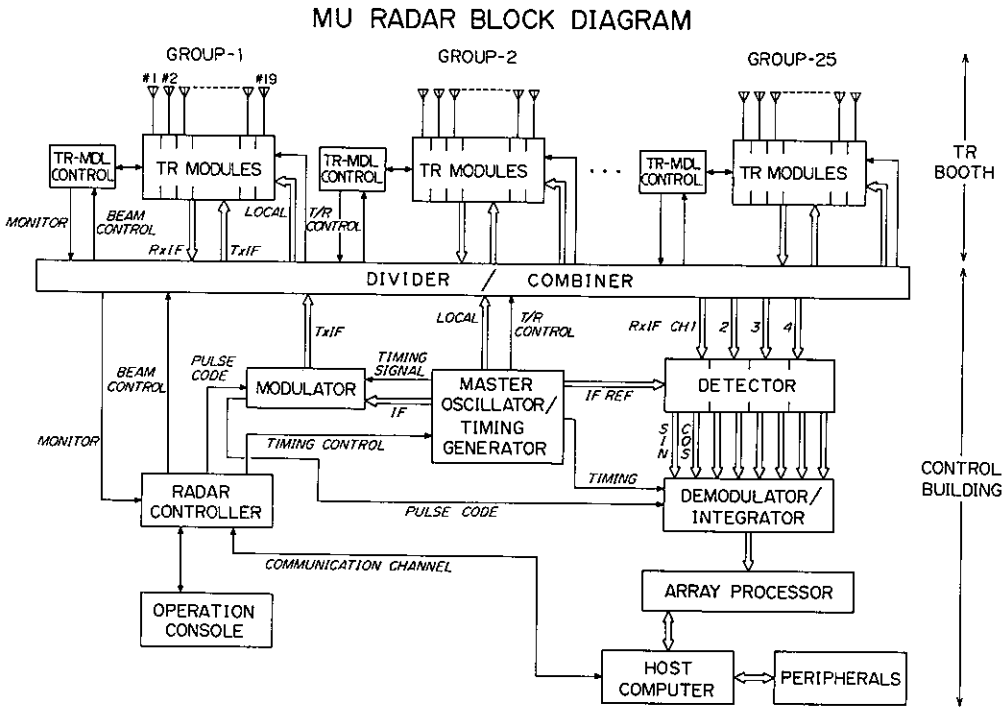

Fig. 2. Block diagram of the MU radar, Shigaraki, Shiga, Japan. The TR modules and TR module controllers (TR-mdl. control) are housed in TR booths built in the antenna field. Other system equipment is installed in the control building [*Kato et al.*, 1984].

TABLE 1. Basic Parameters of the MU Radar (Final System)

Parameter	Value
Location	Shigaraki, Shiga, Japan (34.85°N, 136.10°E)
Radar system	monostatic pulse radar; active phased array system
Operational frequency	46.5 MHz
Antenna	circular array of 475 crossed yagis
aperture	8330 m^2 (103 m in diameter)
beam width	3.6° (one way; half power for full array)
steerability	steering is completed in each IPP
beam directions	1657; 0°–30° off zenith angle
polarizations	linear and circular
Transmitter	475 solid state amplifiers (TR modules; each with output power of 2.4 kW peak and 120 W average)
peak power	1 MW (maximum)
average power	50 kW (duty ratio 5%)(maximum)
bandwidth	1.65 MHz (maximum) (pulse width: 1–512 μs variable)
IPP	400 μs to 65 ms (variable)
Receiver	
bandwidth	1.65 MHz (maximum)
dynamic range	70 dB
IF	5 MHz
A/D converter	12 bits × 8 channels
Pulse compression	binary phase coding up to 32 elements; Barker and complementary codes presently in use

formed inside the TR modules. The signal is transferred at the IF between the control building and the remote TR booths. This way of frequency conversion prevents instabilities in the power amplifier due to possible leakage of output power into the input signal.

An antenna element consists of two orthogonally crossed three-subelement yagis pointed toward the zenith direction. Linear and circular polarizations of any sense are available with the aid of a polarization-selection switch in each TR module.

The overall operation of the MU radar is supervised by a programmable radar controller (the main constituent is a desktop computer HP9835A) linked with the 25 TR module controllers. Various timing signals necessary for real time system control are generated according to instructions from the radar controller. Sophisticated software in the radar controller makes a variety of flexible operations possible. For instance, it is possible to steer the antenna beam in each interpulse period (IPP), i.e., up to 2500 times every second, virtually to any direction within 30° of the zenith. Moreover, it is possible to excite only a portion of the antenna array and receive the echo by other portions and/or to steer multibeams in different directions.

A large amount of data (up to 1024 samples) can be processed in real time. A superminicomputer (VAX-11/750) and an array processor (MAP-300) with a 2-Mbyte random access memory (RAM) are installed for this purpose. Before being processed by the computer, the echo signals are decoded for pulse compression and then coherently integrated for data compression by special purpose hardware.

High reliability of the system is expected to be achieved by means of a network of the radar controller and 25 TR module controllers which monitor the TR modules during operation [*Fukao et al.*, this issue].

3. ANTENNA

3.1. *Array configuration*

The array pattern (or radiation pattern) of a large array is approximated by a product of the array factor and the element pattern. The former is determined by array configuration, while the latter is principally affected by mutual coupling between array elements. The MU radar antenna array is designed subject to the following restrictions:

1. The antenna aperture is to be less than about 100 m in diameter at radar site.
2. The number of antenna elements/TR modules necessary to attain the total peak radiation power of 1 MW is approximately 500, because the output power of each TR module is expected to be about 2 kW.
3. Neither spatial nor electrical tapering is incorporated.

The array configuration is designed to be nearly circular in order to obtain almost symmetric sidelobes with respect to azimuth. The diameter of the array is 103 m (the aperture is 8330 m^2). As for arranging the array elements, a triangular grid is used, since it generally allows a wider range of antenna beam steering than a rectangular grid with the same element density.

The actually constructed antenna array is shown in Figure 3, where 475 array elements indicated by crosses are periodically arranged on the grids of equilateral triangles, with one of their sides pointed to the geographical meridian [*Kato et al.*, 1984]. The two dipoles are mounted in the east-west (EW) and north-south (NS) directions, respectively. The element spacing is 0.7λ (λ is wavelength), for which no

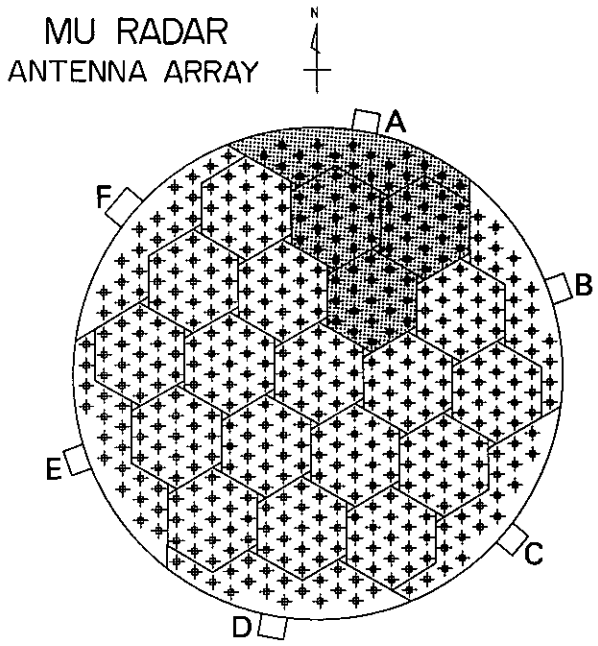

Fig. 3. MU radar antenna array. Each cross represents a crossed three-subelement yagi. The small square at each array element position is a concrete block for the element foundation. The six boxes outside the antenna array, indicated as *A–F*, represent the booths which accommodate the TR modules. All booths except *F* accommodate the TR modules for three hexagonal subarrays and one peripheral subarray. The shaded area shows groups accommodated by booth *A*. The TR modules for the central hexagon are housed in booth *F* [*Kato et al.*, 1984].

grating lobe is formed at beam positions within 40° away from the zenith.

The antenna array can be divided into 25 groups, each consisting of 19 array elements connected to the same number of TR modules. Nineteen of them are identical hexagonal subarrays composing the main part of the antenna array, while the remaining six are subarrays distributed around the periphery making the array nearly circular. Each group can be driven separately, and even individual array elements can be driven independently. However, the maximum number of separate beams is limited to four due to the number of available detector channels [*Fukao et al.*, this issue]. The peak radiation power of 1 MW is attained when all groups are coherently activated.

Figure 4 is a photograph of the actual antenna, showing the overall construction, the control building, and RF cables.

3.2. *Element structure*

Element spacing is related to the antenna gain of the array elements. For the present equilateral triangular grid with sides of 0.7λ ($\simeq 4.5$ m), the element gain g_e is limited by the physical area S that each array element occupies, as

$$g_e \leq 4\pi S/\lambda^2 = 5.30 \quad (=7.24 \text{ dB})$$

Three- or four-subelement yagis have a gain of this order.

The elements have been designed to meet the following requirements:

1. A high front-to-back ratio is required in order to avoid change of array pattern due to variation in the reflectivity of the ground plane.
2. The required bandwidth is more than 1.65 MHz.
3. The antenna impedance should be matched to feed line impedance of 50Ω.

The active impedance and element pattern are examined for crossed yagis with three and four subelements in an infinite array, applying the method of analysis developed for periodic dipole arrays by *Stark* [1966] to the present multisubelement yagi arrays.

The radiator of both yagis is folded in order to cancel the unbalanced current on it. This effect is taken into account by using the geometrical mean distance of the cross section of the folded subelement as its effective radius. This folding works as an impedance transformer, and the input impedance becomes 4 times that of an unfolded antenna. Therefore another impedance transformer, or balun, which reduces the input impedance to a quarter is inserted at the feed point (see section 3.4). Further details of the method of analysis are described elsewhere [*Sato*, 1981; *Fukao et al.*, 1985*b*].

In designing a multisubelement yagi, the parameters to be determined are the length of subelements, spacings between subelements, and their diameters. Since the diameters, as long as they are not too small, do not appreciably affect element properties, the diameters of all subelements are fixed at 2.17 cm, a readily available size of commercial aluminum and steel pipe.

In order to satisfy the requirement for high front-to-back ratio, it has been the intention to design an array element which shows the highest gain in the absence of the ground plane in an infinite array. It has been found through the present analysis that the properties of an array element optimized in the presence of the ground plane is substantially affected by variations in the reflectivity of the ground. Since the amount of energy available from the power supply is kept constant in the present analysis, radiations to

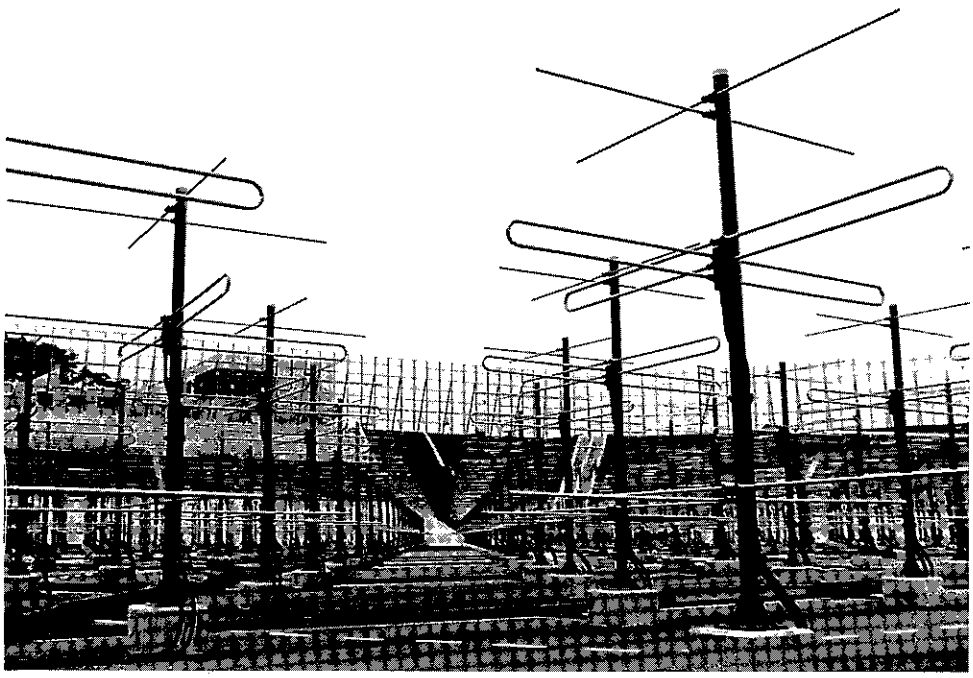

Fig. 4. Photograph taken in the antenna field, showing crossed three-subelement yagis and RF cables.

undesired directions and the reflection at the feed point should become smallest when maximum gain is attained.

The procedure for finding the optimum element dimensions is essentially computing element gain in the infinite array, changing the length and spacing of subelements, and determining the combination which gives the highest gain.

After the procedure has converged a few iterations are performed, taking into account the perfectly conducting ground plane. The modification in the element dimensions by this additional iteration is very small because the properties of the optimized array element are only minimally affected by the ground plane. Figure 5 illustrates the dimensions of the optimized three-subelement yagi and its radiation pattern in an isolated situation. The radiator and reflector/director are made of aluminum and steel pipe, respectively.

In the case of the optimized four-subelement yagi, a higher front-to-back ratio is obtained, but the bandwidth is found to be narrower than that of the three-subelement yagi. Most particularly, the maximum value of the voltage standing wave ratio (VSWR) at the zenith direction exceeds 1.65 compared to 1.25 for the three-subelement yagi. It is also preferable from a economic point of view to choose the element with a fewer number of subelements if all other properties do not differ appreciably.

3.3. *Array pattern*

At a point frequency of 46.5 MHz, the calculated element gain of the three-subelement yagi in the infinite array coincides with the theoretical limit of 7.24 dB in the zenith direction. The active impedance is very close to 50Ω, providing excellent matching to the feed line. The impedance matching is preserved even when the beam direction is tilted as much as 30° away from the zenith. VSWR is always below 1.3 within this range of zenith angle.

Frequency dependence of the element properties is fairly small, and VSWR is kept below 1.25 at the zenith direction within the bandwidth of 1.65 MHz.

Figure 6 shows a computed array pattern for three different beam directions using optimized three-subelement yagis as array elements. Only the NS-aligned elements are excited, and the beam is changed in the meridional (NS) plane. The beam width of the main lobe is approximately 3.6°, corresponding to a gain of 34 dB. The first side lobe is suppressed by more than 18 dB with respect to the main lobe. The spillover radiation at elevation angles below 20° is reduced by more than 40 dB even when

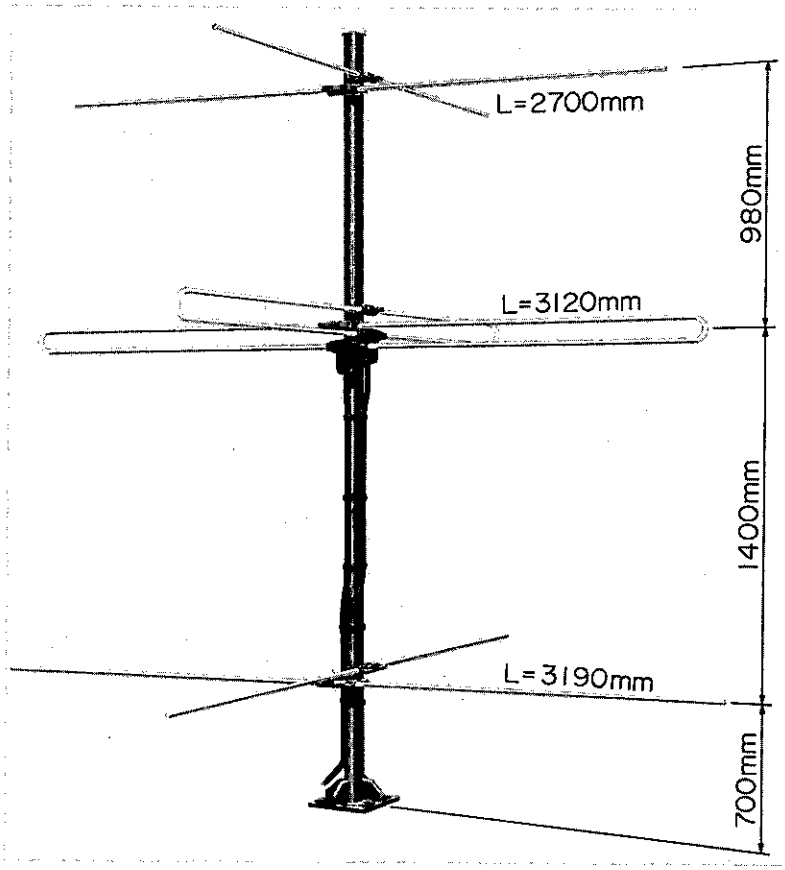

Fig. 5a. Optimized crossed three-subelement yagi.

the antenna beam is tilted 30° from the zenith. It is found that in the azimuth directions the sidelobes are distributed almost symmetrically and uniformly without any outstanding peak in any particular direction.

The theoretical beam width is approximately 17.3° for a single hexagonal subarray, and 9.0° for a combination of three hexagonal subarrays.

Deterioration of element properties due both to the edge effect and to the current flowing on the antenna mast is considered to be negligibly small [*Fukao et al.*, 1985*b*, *c*].

3.4. *Feed point structure*

The antenna feed point is molded in a waterproof box of synthetic resin. The detailed structure is shown in Figure 7. The coiled coaxial cable inside is a half wavelength balun which reduces the input impedance to a quarter of that without it.

The current flows from *A* in the inner coaxial conductor through *B* into both the folded dipole terminal *C* and one terminal of the balun *D*. It appears at the second balun terminal *E* in opposite phase and feeds the other dipole terminal *F*. Outer coaxial conductors for both feeder and balun, indicated by *G* and *H*, respectively, are connected to *I* and earthed at *J* to the antenna mast.

Insertion of the balun transforms the antenna impedance from 200Ω to $50.7 + j1.5\Omega$ to enable the input impedance of the feed point to match the feed line impedance of 50Ω. The optimization mentioned in section 3.2 is performed again to attain this modified impedance. As a consequence, the length of the radiator becomes 2 cm longer, and the spacings between radiator and reflector/director are altered by +1 cm and −4 cm, respectively, in comparison with those without the balun. However, the resultant changes in the element properties are found to be very small. The antenna element shown in Figure 5 takes this modification into account.

4. TRANSMITTER-RECEIVER MODULE

As described above, both upconvert and downconvert are conducted in the remote booths, so that the

IF (5 MHz) and local (41.5 MHz) signals are transferred between the booths and the control building. The signals are then sent to each booth via AF coaxial cables of equal length. (AF is an abbreviation used for coaxial cables which employ an aluminum outer conductor and are insulated with foamed polyethylene). Upon arrival at the booth, the signals are divided into four (or five) groups by the TR module divider (TX IF divider and local divider, respectively) and distributed to the 19 TR modules in each of the groups.

On the other hand, the received IF signals from the 19 TR modules are combined into one by the TR-module combiner (RX IF combiner) and sent directly to the control building. Figure 8 is a block diagram of one group of TR modules. The timing signals for T/R switching and initial set pulse (ISPL) are split in the same way.

The main constituents of the TR module are a mixer (MIX) unit and a power amplifier (PA) unit, whose block diagrams are shown in Figures 9 and 10, respectively. Control signals are indicated by thin arrows. Frequency conversion is performed in the MIX unit. The 41.5 MHz local signal (LO) fed to the MIX unit passes through a digital phase shifter for beam steering and TX/RX phase correction as will be shown later. The MIX unit also contains a buffer amplifier, a gate for transmission, and preamplifier for reception.

The PA unit amplifies the RF (46.5 MHz) signal supplied from the MIX unit up to 63.7 dBm (2350 W), and feeds it to an array element. An exciter con-

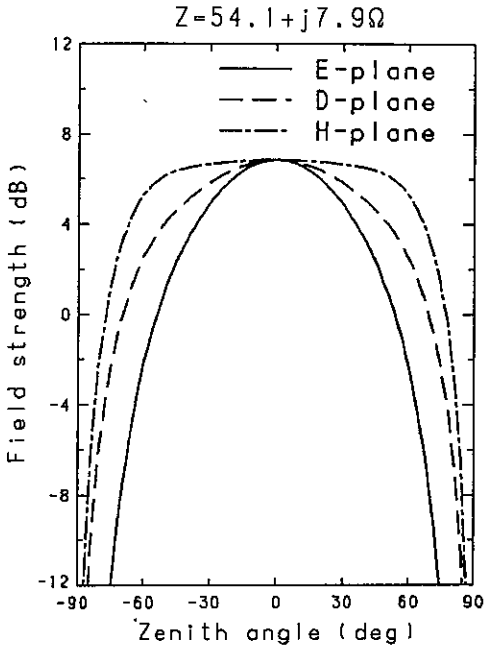

Fig. 5b. Computed radiation pattern of a single isolated yagi. The input impedance is $54.1 + j7.9\Omega$, in contrast to the active impedance of around 50Ω in the MU radar antenna array. The field strength is normalized to the radiation field of an isotropic antenna matched to the feed line impedance. Solid, dashed, and dotted-dashed curves show the vertical plane patterns in the directions parallel (*E* plane), diagonal (*D* plane) and perpendicular (*H* plane) to excited dipole, respectively.

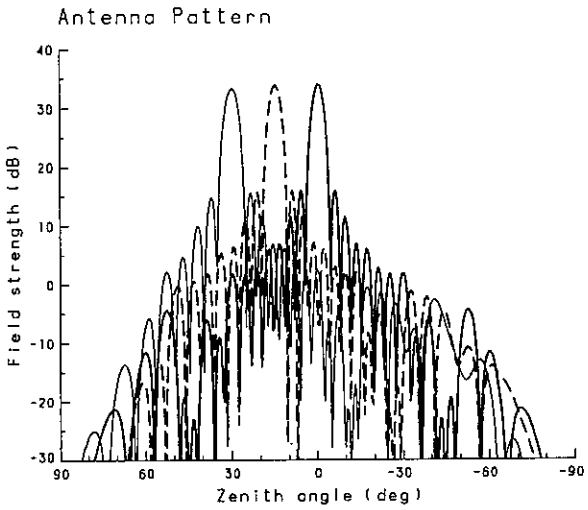

Fig. 6. Computed radiation patterns of the MU radar antenna employing optimized three-subelement crossed yagi as array elements. Only the NS-aligned elements are excited. The field strength is normalized to the radiation field of an isotropic antenna matched to feed line impedance. The antenna beam is tilted by 0° (zenith), 15°, and 30° from the zenith along the NS direction.

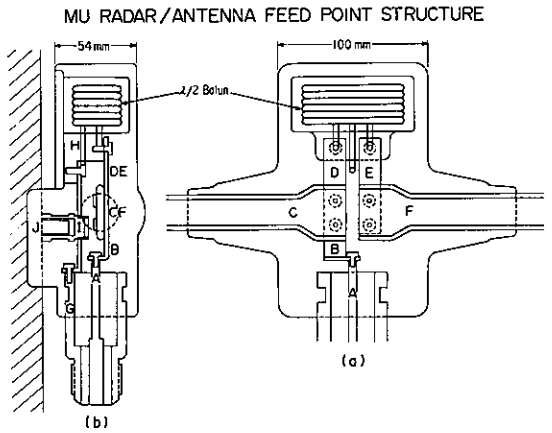

Fig. 7. Structure of antenna feed point. *C* and *F* are the terminals of the radiator (folded dipole) of a three-subelement yagi, while *D* and *E* are the ports of the $\lambda/2$ balun. *A* and *G* are the inner and outer coaxial conductors, respectively, and *H* is the outer conductor of the balun.

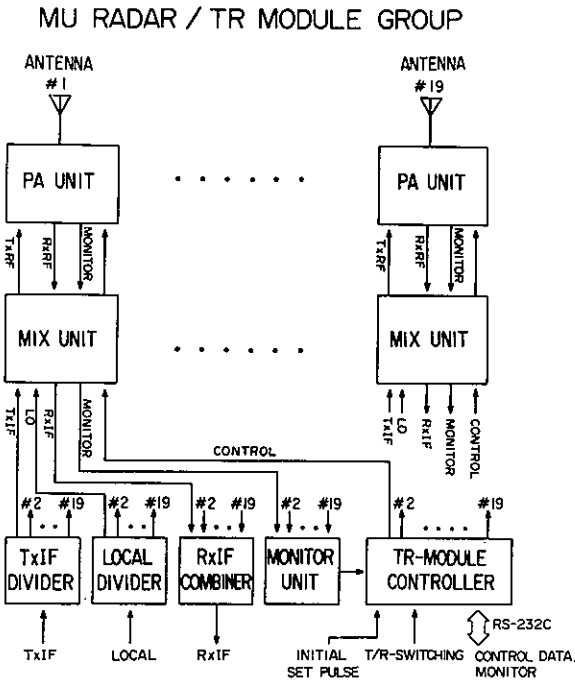

Fig. 8. Block diagram of one group of TR modules. Nineteen array elements and the same number of TR modules constitute one group, with common equipment consisting of TR module divider/combiner, monitor unit, and TR module controller.

sisting of a three-stage amplifier operates in A class with a gain of 39.5 dB. The final power amplifier stage is composed of four push-pull circuits operating in parallel mode with a gain of 12 dB. Eight high-power transistors (TH-430) are employed.

A TR switch consists of a combination of two 3-dB hybrids and high-power PIN diodes [e.g., *Czechowsky et al.*, 1984]. Three additional diode switches are inserted in the RX channel in order to obtain a total isolation of 100 dB between TX and RX signals. Switching requires 10 μs, limiting the time for TX and sampling start.

A bandpass filter is inserted after the TR switch to prevent transmission of unnecessary harmonics. The second and third harmonics are reduced by 85 dB and more than 90 dB, respectively, in comparison with the fundamental frequency.

Phase and intensity of the TX signal are monitored by TR module controller via a directional coupler. During observation, the radar controller polls the TR module controller for monitor data. Also, output VSWR is detected by the hardware in order to protect high-power transistors. The polarization (selection) switch is comprised of two relays and a 3-dB hybrid, and gives two linear as well as right-hand and left-hand circular polarizations. The signal level at three points and gain of both exciter and final power amplifier are tabulated at the bottom of Figure 10. The overall gain of the PA unit is approximately 50 dB.

Figure 11 shows the input-versus-output characteristics of the PA unit measured at four points: output of the exciter, a combined signal of two push-pull circuits, an input of the TR switch, and a final output of the polarization switch. The maximum output power is 2350 W for a signal of 13 dBm at the input port of the exciter when a linear polarization is selected. As for the curve d, the output increases linearly up to the maximum value, and saturates if the input signal level exceeds 13 dBm, a phenomenon attributable to the action of the automatic power control circuit. The linearity is preserved more than 20 dB below the nominal input level of 13 dBm. Within this input range the phase varies no more than 2°–3°. When feeding cable loss is taken into consideration, the final radiation power from each antenna element becomes 2100 W. The maximum radiation power of approximately 2000 W is provided for both circular polarizations. Chassis dimensions are 60 cm H × 14 cm W × 55 cm D. A photograph and a rough sketch of a PA unit are shown in Figures 12*a* and 12*b*, respectively.

5. FEEDING NETWORK

The IF and local signals which are divided into 6 by the divider in the control building are sent underground via AF coaxial cables to the booths in the antenna field. As mentioned in section 4, they are split into four (or five) groups in each booth and then

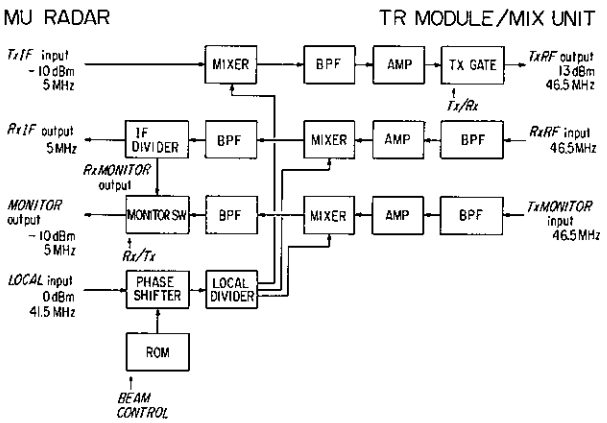

Fig. 9. Block diagram of the mixer (MIX) unit in a TR module.

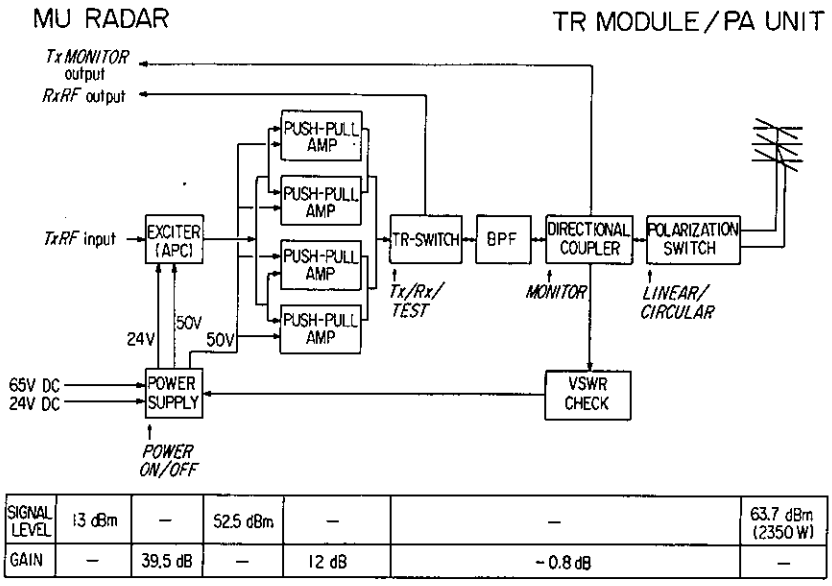

SIGNAL LEVEL	13 dBm	—	52.5 dBm	—	—	63.7 dBm (2350 W)
GAIN	—	39.5 dB	—	12 dB	−0.8 dB	—

Fig. 10. Block diagram of the power amplifier (PA) unit in a TR module. Signal level and gain measured at a few stages are shown in the chart at the bottom.

fed to the individual TR modules. All cables leading to the TR modules are of equal length.

The RF outputs of the TR modules are sent to array elements through AF coaxial cables branched in a tree structure as illustrated in Figure 13. Cable length varies, the longest being 77 m and the shortest 11 m. As a result, both delay time and phase rotation differ in the individual cables. Therefore cable impedance (phase) as observed from the output port of the polarization switch differs among cables even if the input impedance to all yagis is identical. The situation is quite different from that in existing MST radars which have passive phased array systems.

These differences are compensated for in the following way. First, the phase of a reflected wave is measured at the output port of the polarization switch leaving the other cable end short, and then adjusted to make the value equal. This is done by adjusting the "electrical" length in integral multiples of $\lambda/2$ by the addition of a short auxiliary cable. As a result of this adjustment, VSWR is measured to be less than 1.30 within the bandwidth for all array elements.

The delay time differs by 250 ns between the longest and the shortest cables. This difference is compensated for by inserting delay lines into both the TX IF and RX IF channels so that the delay time is equal to that of the longest cable. This compensation is made in steps of 50 ns, a unit fine enough not to deteriorate the array pattern.

Finally, the phase differences among array elements which is caused primarily by individual differ-

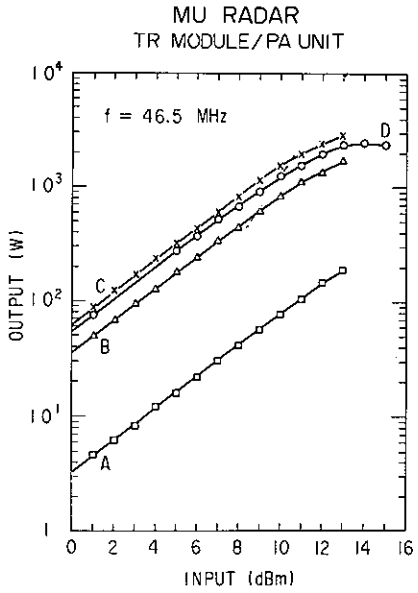

Fig. 11. Input-versus-output characteristics of a standard PA unit. Curves a, b, c and d correspond to an output of the exciter, the combined signal of two push-pull circuits, the input signal of the TR switch and the final output of the polarization switch.

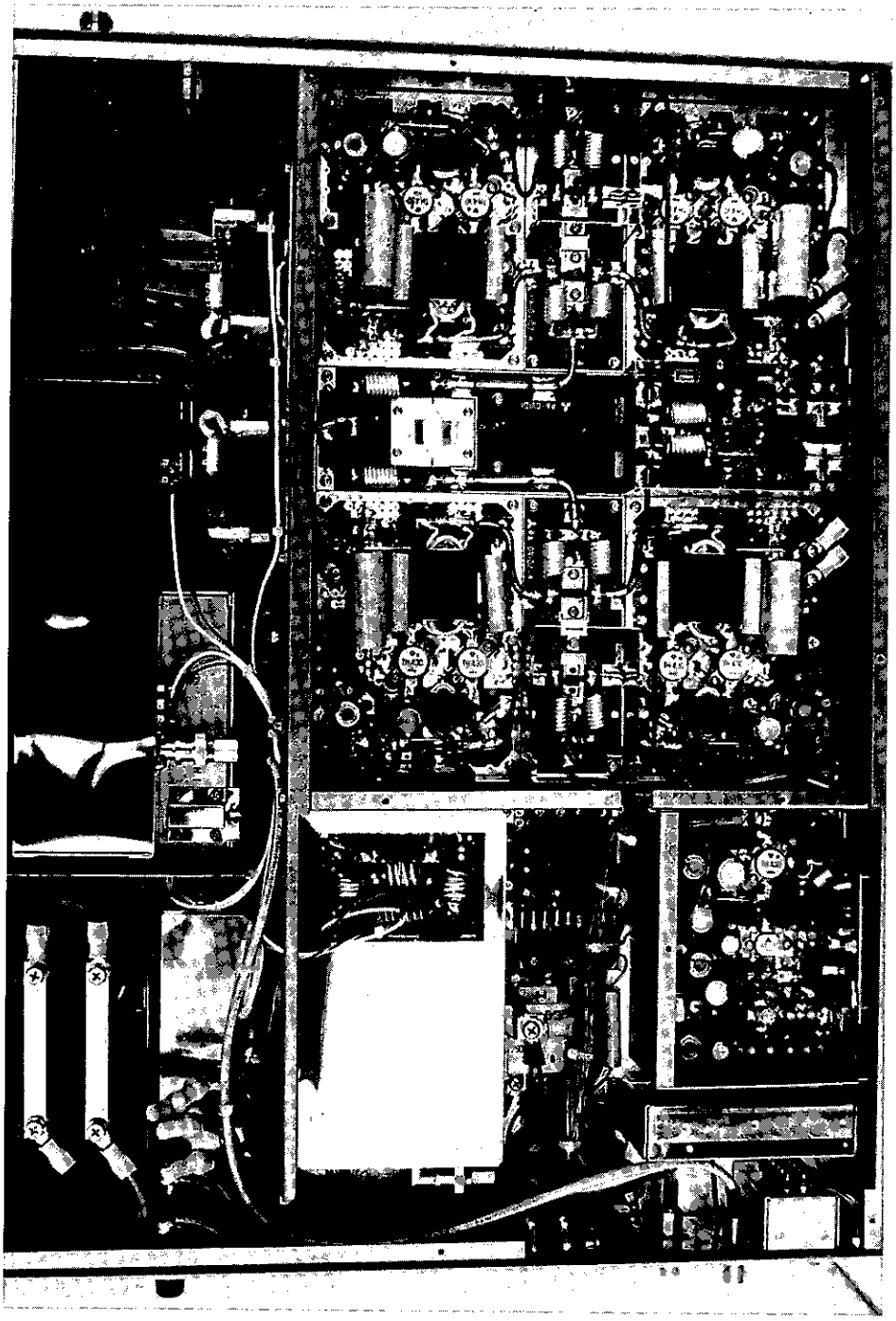

Fig. 12*a*. Photograph of the PA unit in a TR module.

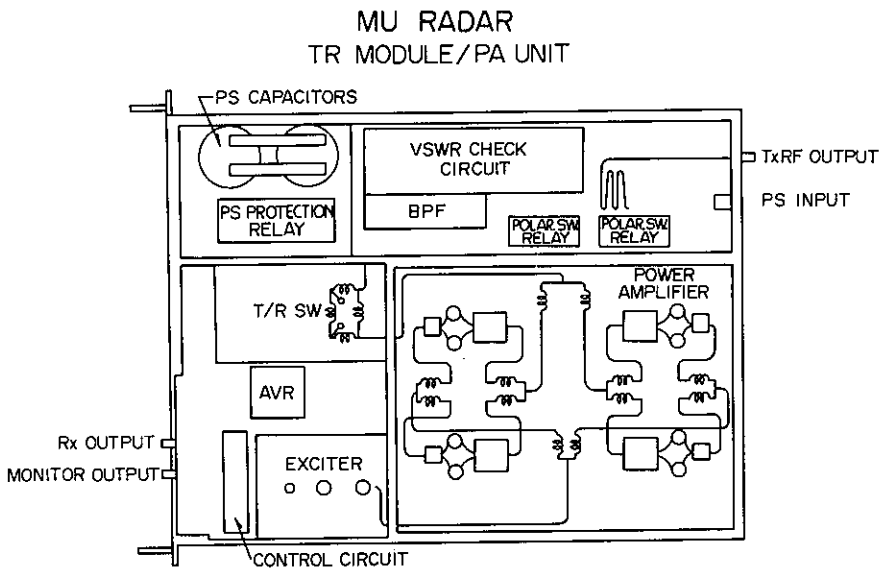

Fig. 12*b*. Rough sketch of Figure 12*a*. Only the main constituents are shown. The eight small circles in the power amplifier box represent the TH-430 high-power transistors composing four push-pull circuits. The smaller and larger squares in the same box represent the input and output transformers, respectively.

ences among the TR modules is equalized by adding proper phase rotation to the TX and RX channels. For TX phase correction, the overall phase rotation is measured for all 475 array elements by comparing the phase of the radiated waves with that of the reference signal. The radiated wave is picked up by a small coil, and then modulated to a photo signal, then guided to the booth and detected by a photo diode. The same measurement is conducted for RX phase correction by means of an RF signal sent to the antenna elements, exchanging the photo modulator for the demodulator. Phase correction values are measured for four different polarizations.

The phase correction data for both TX and RX channels are sent from the radar controller and stored in the one-word RAM in the TR module controller prior to observation. By using this correction data, all antenna elements are fed in an equal phase and the antenna beam is directed toward the zenith.

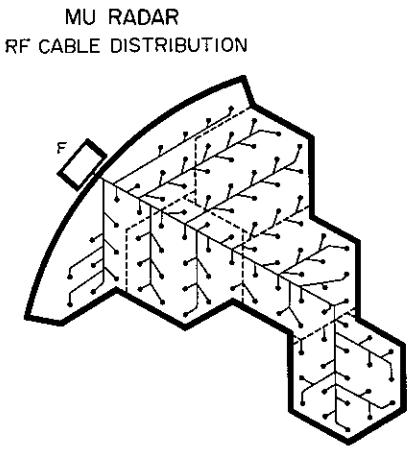

Fig. 13. The RF cable distribution for the five groups in booth *F*.

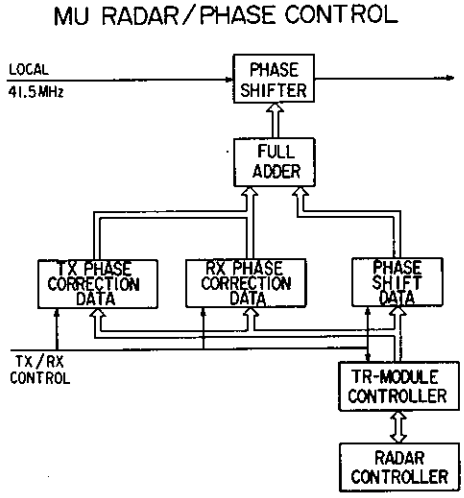

Fig. 14. The basic phase control concept of the MU radar. Phase shift data is used for beam steering, while TX/RX phase correction data are required to compensate for phase differences caused by individual differences in the power amplifiers, varying cable lengths, etc.

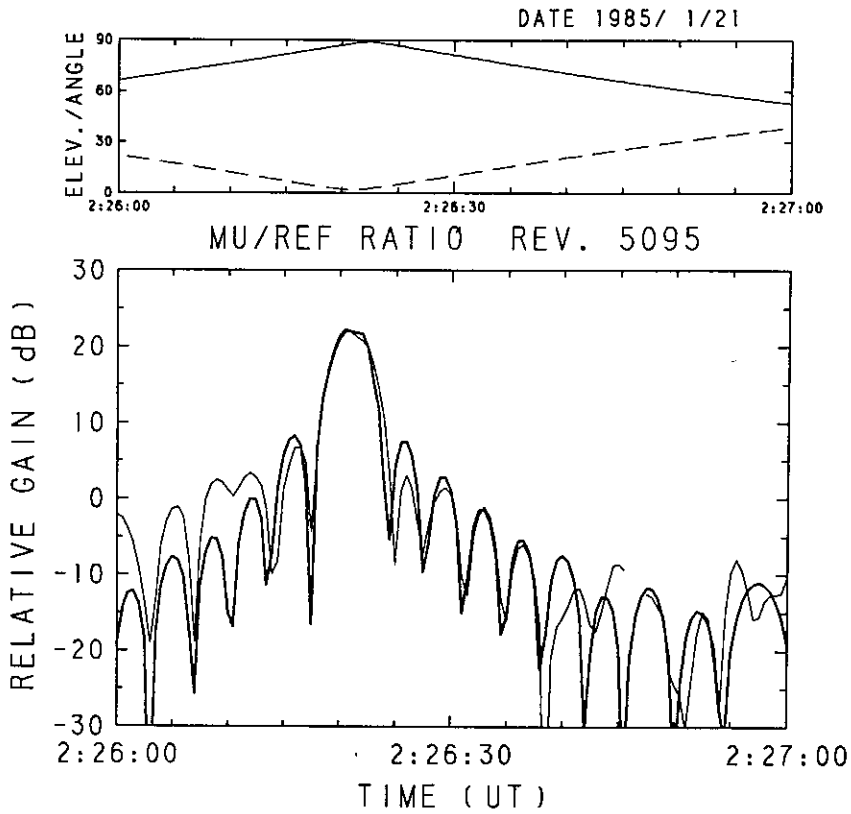

Fig. 15. (bottom) An example of the MU radar TX array pattern (thin line) measured by using the Japanese satellite OHZORA, and the corresponding theoretical antenna gain (thick line) relative to the reference antenna. The reference antenna has almost constant gain for the elevation angles shown in this diagram. (top) Elevation angle of the satellite seen from the MU radar (solid line) and the angle between the direction of the satellite and the axis of the main beam of the MU radar antenna (dashed line) versus time.

The basic phase control concept is shown in Figure 14. All phase shift data required for beam steering are stored in the ROM (read-only memory) installed in the MIX unit of each TR module. They are read out according to instructions from the TR module controller and added alternately either to the TX or RX phase correction data by an 8-bit binary adder following the timing of the T/R switching signal. The output of the adder switches the 8-bit phase shifter.

The phase shifter is essentially the same type as employed for the SOUSY radar [*Schmidt et al.*, 1979; *Czechowsky et al.*, 1984], but it is composed of eight coaxial cables with lengths of $\lambda/2^n (n = 1, 2, \cdots, 8)$. The phase can be changed in steps of $\lambda/256$ or 1.4°. This causes the beam to be steered in the zenith direction in steps of 1° up to 16° from the zenith, in 2° steps in the 16°–30° zenith range, and in 5° steps in the azimuth direction. The total number of beam directions is 1657.

6. SYSTEM CALIBRATION

For passive phased arrays whose TX and RX radiation patterns are reciprocal, both array patterns can be known ordinarily just by measuring the pattern in the receiving mode. By using radio stars, this measurement is actually executed by many MST radars [e.g., *Czechowsky et al.*, 1984]. On the other hand, the TX/RX array patterns of an active phased array are inseparably related to the distributed transmitters and receivers (Figure 1). It is impossible to know the array pattern of the MU radar independently of the TR modules.

Since precise phase alignment of each array element is crucial to realize the desired array pattern, careful calibration of the output phase of each power amplifier and array element is performed by the method mentioned in section 5. As a consequence, the phase is considered to be equalized with an accuracy to 1.4°. The output power of the TR modules

varies no more than 0.1 dB. In this sense, standardization of the TR modules as well as the array elements seems to be quite successful.

It is also necessary to confirm the total performance by measuring the radiation pattern of the whole array from distant locations where the antenna far field condition exists. One test was made by using Cassiopeia A, which is the most intense point source detectable by the MU radar. The received power maximum was observed at an expected time and zenith angle, confirming the proper steering of the antenna beam. The measured beam width coincides with the theoretical value of 3.6°. Also, upon completion of the system, the RX array pattern in the zenith direction was tested by using a CW beacon on board an airplane passing over the MU radar antenna array at an altitude of 5200 m, showing the same result.

The TX array pattern in the zenith direction was also calibrated for a full-power pulse transmission by using a field intensity meter on board the same airplane. In spite of difficulties involved in performing this calibration, such as accurate piloting of the aircraft, the gain and the beam width were found to be close to the theoretically expected values. The first side lobe is suppressed by more than 17.5 dB with respect to the main lobe at the zenith beam position.

Currently, the array pattern is frequently being monitored by using the Japanese satellite OHZORA (a Japanese word which means "the firmament") by means of a 300-W CW signal transmitted from both the MU radar and a reference transmitter at the frequency of 46.5 MHz + 50 kHz [*Fukao et al.*, 1985*a*]. An array pattern along a plane which contains the satellite orbit is measured during one passage of the satellite. The bottom diagram of Figure 15 gives the theoretical (thick line) and measured (thin line) relative gains of the MU radar. The antenna beam is pointed to the apex (the point where the elevation angle of the satellite becomes maximum) of the expected satellite path, i.e., to 3.0° zenith and 140° azimuth. Since the actual satellite path was found by a later analysis to be 1.0° off from the zenith, this figure shows a cross-sectional pattern at 2° off from the main lobe peak. Figure 15 shows that both main beam direction and gain are in close agreement with the theoretical values. However, although the positions of the side lobes are in relatively close agreement down to the lower elevation side lobes, the side lobe levels show a discrepancy of ±5–10 dB between the theoretical and measured patterns. This difference seems to suggest that slightly larger random phase errors still remain in the individual power amplifiers and/or array elements of the MU radar. Apparently, more detailed and continuous monitoring of the array pattern, as well as careful calibration of the individual amplifiers (TR modules) and array elements, is necessary before optimum system performance can be achieved.

7. CONCLUDING REMARKS

The present paper describing the antenna and power amplifiers of the VHF band MU radar shows that it is possible to realize an active phased array system in the VHF band by using available commercial equipment and devices. The in-house equipment related to transmission, reception, on-line data processing, and system control is referred to in the accompanying paper [*Fukao et al.*, this issue].

The antenna beam has been demonstrated to steer every IPP virtually to any direction within 30° from the zenith with very little deterioration of the radiation pattern. All practical requirements for successful operation of the system have been met.

To this date, three groups of 57 TR modules installed first in 1982 have survived 2 years with surprisingly few problems. It is expected that the MU radar will serve for many years to come as an important research tool in the investigation of the three-dimensional structures formed by fast dynamical processes occurring in the middle atmosphere.

Acknowledgments. The authors are indebted to the staff of the Radio Atmospheric Science Center and Department of Electrical Engineering, Kyoto University, for their helpful support. Thanks are also due to W. E. Gordon, Rice University, Houston, Texas, for his suggestions and continuous encouragement. The MU radar is operated by the Radio Atmospheric Science Center of Kyoto University.

REFERENCES

Balsley, B. B., and K. S. Gage, The MST radar technique: Potential for middle atmospheric studies, *Pure Appl. Geophys., 118*, 452–493, 1980.

Balsley, B. B., and K. S. Gage, On the use of radars for operational wind profiling, *Bull. Am. Meteorol. Soc., 63*, 1009–1018, 1982.

Czechowsky, P., G. Schmidt, and R. Rüster, The mobile SOUSY Doppler radar: Technical design and first results, *Radio Sci., 19*, 441–450, 1984.

Fukao, S., S. Kato, T. Aso, M. Sasada, and T. Makihira, Middle and upper atmosphere radar (MUR) under design in Japan, *Radio Sci., 15*, 225–231, 1980.

Fukao, S., T. Sato, and S. Kato, Monitoring of the MU radar antenna pattern by satellite OHZORA (EXOS-C), *J. Geomagn. Geoelectr., 37*, 431–441, 1985*a*.

Fukao, S., T. Sato, H. Hojo, I. Kimura, and S. Kato, A numerical consideration on edge effect of planar dipole phased arrays, *Radio Sci.*, in press, 1985*b*.

Fukao, S., T. Sato, H. Hojo, I. Kimura, and S. Kato, Effects of antenna element structure on element properties and array pattern of a planar phased array, *Radio Sci.*, in press, 1985*c*.

Fukao, S., T. Tsuda, T. Sato, S. Kato, K. Wakasugi, and T. Makihira, The MU radar with an active phased array system, 2, In-house equipment, *Radio Sci.*, this issue.

Gage, K. S., and B. B. Balsley, MST radar studies of wind and turbulence in the middle atmosphere, *J. Atmos. Terr. Phys.*, *46*, 739–753, 1984.

Green, J. L., K. S. Gage, and T. E. VanZandt, Atmospheric measurements by VHF pulsed Doppler radar, *IEEE Trans. Geosci. Electron.*, *GE-17*, 262–280, 1979.

Harper, R. M., and W. E. Gordon, A review of radar studies of the middle atmosphere, *Radio Sci.*, *15*, 195–211, 1980.

Kato, S., T. Ogawa, T. Tsuda, T. Sato, I. Kimura, and S. Fukao, The middle and upper atmosphere radar: First results using a partial system, *Radio Sci.*, *19*, 1475–1484, 1984.

Klostermeyer, J., and R. Rüster, VHF radar observation of wave instability and turbulence in the mesosphere, *Adv. Space Res.*, *4*, 79–82, 1984.

Larsen, M. F., and J. Röttger, VHF and UHF Doppler radars as tools for synoptic research, *Bull. Am. Meteorol. Soc.*, *63*, 996–1008, 1982.

Röttger, J., The MST radar technique, in *Handbook for MAP*, vol. 13, edited by R. A. Vincent, pp. 187–232, University of Illinois, Urbana, Ill., 1984.

Sato, T., Coherent radar measurement of the middle atmosphere and design concepts of MU radar, Ph.D. thesis, Dep. of Electr. Eng., Kyoto Univ., Kyoto, Japan, 1981.

Schmidt, G., R. Rüster, and P. Czechowsky, Complementary code and digital filtering for detection of weak VHF radar signals from the mesosphere, *IEEE Trans. Geosci. Electron.*, *GE-17*, 154–161, 1979.

Stark, L., Radiation impedance of a dipole in an infinite planar phased array, *Radio Sci.*, *1*, 361–377, 1966.

S. Fukao, Department of Electrical Engineering, Kyoto University, Yoshida, Kyoto 606, Japan.

S. Kato, T. Sato, and T. Tsuda, Radio Atmospheric Science Center, Kyoto University, Uji, Kyoto 611, Japan.

T. Makihira, Communication Equipment Works, Mitsubishi Electric Corporation, Amagasaki, Hyogo 661, Japan.

K. Wakasugi, Department of Electrical Engineering, Kyoto Institute of Technology, Matsugasaki, Kyoto 606, Japan.